Food Chemistry: X 21 (2024) 101089

Contents lists available at ScienceDirect

Food Chemistry: X

journal homepage: www.sciencedirect.com/journal/food-chemistry-x

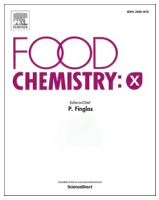

Oxidized konjac glucomannan: A safe dietary fiber influencing mouse gut microbiota

Yao Li [a,b,1], Hongjia Lu [c,1], Chao Liao [b,d], Xiong Liu [b,*]

[a] College of Food Science and Engineering, Hainan University, Haikou 570228, China
[b] College of Food Science, Southwest University, Chongqing 400715, China
[c] College of Landscape Architecture and Life Science, Chongqing University Of Arts and Sciences, Chongqing 402160, China
[d] Quality Supervision Center of Wuliangye Co. Ltd., Sichuan 644000, China

ARTICLE INFO

Keywords:
Oxidized konjac glucomannan
Gut microbiota
Oral toxicity

ABSTRACT

In this 13-week study, the potential effects of oxidized konjac glucomannan (OKGM) on ICR mice's metabolic health and gut microbiota were investigated and contrasted with enzyme-hydrolyzed KGM (EKGM) at a same molecular weight. Mice were fed diets containing 0 %, 2.5 %, 5.0 %, and 7.5 % of OKGM for 13 weeks. Results indicated that OKGM induced no adverse effects, with overall health, body weight gain, food consumption, and clinical pathology parameters being comparable to the control group. The no-observed-adverse-effect-level for OKGM was determined at 7.5 % in the diet, corresponding to 10.21 and 12.01 g/kg/day for male and female mice, respectively. OKGM intake positively regulated gut microbiota, characterized by a reduction in the relative abundance of *Firmicutes*, an increase in *Bacteroidetes*, and an enhanced presence of *Lactobacillus*, particularly *Lactobacillus reuteri*. In comparison, EKGM differently modulated the microbiota, notably increasing *Muribaculaceae*. These findings suggest that OKGM has the potential to be a functional food additive.

1. Introduction

Konjac glucomannan (KGM), a naturally occurring heteropolysaccharide, is predominantly found in the tubers of Amorphophallus Konjac. Its structural backbone is characterized by β-1,4 glycosidic bonds, interlinking D-mannose and D-glucose units, and features an acetyl group at the C-6 position on roughly every 19th sugar unit (Jian, Tu, Wu, Xiong, Pang, & Sun, 2017). KGM, known for its prebiotic impact on intestinal health, is extensively utilized in various solid and viscous food products. However, the inherent high viscosity of native KGM hampers its dissolution in water, especially at high concentrations, thus limiting its application in food processes involving liquid or beverage formulations. To overcome this, degradation methods are commonly employed to enhance water solubility and reduce viscosity. Furthermore, studies have indicated that depolymerized KGM exhibits enhanced benefits for gut microbiota when compared to its native form (Yin, Ma, Xie, Nie, & Wu, 2020). Consequently, researchers have developed a variety of techniques for depolymerizing KGM, including oxidative degradation, ultrasonic degradation, acidic hydrolysis, and enzymatic hydrolysis, among others (Jian et al., 2017; Jin et al., 2014; Li, Li, Geng, Song, & Wu, 2017). Among these degradation techniques, oxidative reactions are particularly effective in depolymerizing KGM, as they break glycosidic bonds and alter chemical group structures. Specifically, during oxidative degradation, some hydroxy groups in the KGM glucose or mannose units are transformed into aldehyde groups and carboxyl groups (Chen et al., 2016; Yu, Lu, & Xiao, 2007). The generated reactive aldehyde and carboxyl groups offer OKGM a structural basis to become a macromolecular cross-linking agent. Accordingly, oxidized KGM has drawn much attention for being applied in target delivery systems for controlled release of drugs, such as hard capsules, microspheres, composite hydrogels and polymer films (Chen et al., 2016; Korkiatithaweechai, Umsarika, Praphairaksit, & Muangsin, 2011; Lu et al., 2015). In these studies, the OKGM was usually prepared by sodium periodate, hydrogen peroxide, and sodium hypochlorite. Compared with those oxidizing agents, ozone emerges as a more efficient and environmentally friendly oxidizing alternative (Espino-Perez, Gilbert, Domenek, Brochier-Salon, Belgacem, & Bras, 2016).

In a previous work, the OKGM with a low viscosity was prepared by the ozone treatment (Li, Liu, Xie, Shabani, & Liu, 2021). Besides, the prepared OKGM showed the potential to improve the feces gut

* Corresponding author at: No. 2 Tiansheng Road, Beibei District, Chongqing 400715, China.
E-mail address: liuxiong848@hotmail.com (X. Liu).
[1] Yao Li and Hongjia Lu contributed equally to this paper.

https://doi.org/10.1016/j.fochx.2023.101089
Received 20 September 2023; Received in revised form 12 December 2023; Accepted 18 December 2023
Available online 21 December 2023

microbiota by an in *vitro* fermentation experiment (Li, Gong, Lu, Ma, & Liu, 2023). Despite this, in *vivo* studies exploring OKGM's effects on gut microbiota remain limited. OKGM presents a promising opportunity for development as a healthy dietary supplement, enhancing foods with its prebiotic functions. While ozone's breakdown into atmospheric oxygen minimizes hazardous residues, ensuring the safety of OKGM as a novel food additive necessitates comprehensive assessments. Currently, there is a scarcity of detailed safety evaluations of OKGM. It is anticipated that, if proven non-toxic, OKGM could beneficially regulate gut microbiota.

This work aimed to assess the feasibility of using OKGM in foods. Effects of OKGM on metabolic health was evaluated by a 13-week oral toxicity study in ICR mice, in compliance with OECD Guideline 408 (OECD, 1998). This research is unique as it not only investigated the influence of OKGM on gut microbiota but also compared its effects with those of enzyme-hydrolyzed KGM (EKGM) at similar molecular weight. The findings from this study are poised to offer critical insights into the oral safety profile of OKGM, marking a significant advancement in the understanding of its use as a dietary supplement.

2. Materials and methods

2.1. Material

Purified KGM with a purity of 95 % was procured from Shiyan Huaxianzi Konjac Products Co., Ltd (Hubei, China). The basic diet for the mice consisted of powdered fodder provided by Jiangsu Xietong Pharmaceutical Bioengineering Co., Ltd, China. Food-grade pre-gelatinized corn starch was obtained from Dezhou Gaofeng Starch Co., Ltd, China. The reagents including acetic acid, propionic acid, butyric acid, valeric acid, *n*-butyric acid, and i-valeric acid were procured from Aladdin (Shanghai, China) with all other chemicals being of analytical grade. Deionized distilled water was used consistently in all experimental procedures. The samples of OKGM and EKGM, with average molecular weights of 1.65×10^5 and 1.73×10^5 Daltons respectively, were prepared as per the methodology outlined in Li et al. (2023). Detailed compositions of OKGM and EKGM, as well as the potential structural alterations post-degradation, are depicted in Table S1 and Fig. S1, respectively.

2.2. Experimental animals and maintenance

Specific-pathogen-free male and female ICR mice were procured from Hunan Slyke Jingda Experimental Animal Co., Ltd. They underwent a one-week acclimatization to laboratory conditions. At the experiment's outset, these five-week-old mice had body weights within 24–26 g for males and 22–24 g for females. The mice were randomly divided into ten groups, each consisting of 12 males or females (three per cage), forming various experimental groups: Control Male (CM), Low-Dose OKGM Male (LOKM), Medium-Dose OKGM Male (MOKM), High-Dose OKGM Male (HOKM), EKGM Male (EKM) for males; and Control Female (CF), Low-Dose OKGM Female (LOKF), Medium-Dose OKGM Female (MOKF), High-Dose OKGM Female (HOKF), EKGM Female (EKF) for females. Housed in a controlled environment with temperatures of 22–26 °C, relative humidity between 40 and 70 %, and a 12-hour light/dark cycle, these mice resided in polycarbonate cages with constant air exchange. Bedding comprised wood shavings from Lepeter Biotechnology Co., Ltd, Chongqing, China. Mice had unrestricted access to feed and purified drinking water, except during pre-necropsy overnight fasting. This study, approved by the Institutional Animal Care and Use Committee of Southwest University (Approval number: IACUC-20210225-03), adhered to the EU Directive 2010/63/EU for animal experiments, ensuring ethical and scientific validity.

2.3. Preparation of test diets

The experimental diets were formulated by enriching the basal diet with OKGM and pregelatinized corn starch. These diets were tailored with varying concentrations of OKGM: 2.5 % for low dose, 5.0 % for mid dose, and 7.5 % for high dose, by weight. To maintain consistency, the low and mid dose diets were balanced with corn starch to achieve a total of 7.5 % additive content. The control diet comprised the basal diet supplemented with 7.5 % pregelatinized corn starch, equalizing the total additive level across all diet groups. The powdered OKGM with the feed was meticulously blended using a high-speed mixer and then extruded the mixture into rod-shaped pellets at room temperature. The experimental diets, inclusive of various OKGM percentages (0 %, 2.5 %, 5.0 %, and 7.5 %), were prepared on a weekly basis. Similarly, the EKGM diet, constituting 5.0 % EKGM, was prepared following the same method. Prior to administration, all freshly prepared diets were stored at 4 ℃ in airtight, sealed plastic containers in a cold room.

2.4. Experimental design and methods

Body weight and physical examinations were recorded and performed weekly from the start of the treatment period (Day 1) to the day of scheduled necropsy. The weekly feed consumption per cage was determined by weighing the supplied and leftover feed from Day 1 to Day 91. The OKGM intake per kilogram of body weight was calculated using the nominal dietary levels of OKGM, the feed intake, and the body weight. Feed conversion efficiency (%) $= \frac{Weeklybodymassgain(g)}{Weeklyfoodconsumption(g)} \times 100$

Blood samples were obtained from the mice on the day of scheduled necropsy via the eyeball removal method. Heparin sodium was used as anticoagulant. A Mindray BC-2600Vet Hematology System (Shenzhen, China) was applied to measure red blood cell parameters (Hematocrit (HCT), red blood cell count (RBC) and mean corpuscular hemoglobin concentration (MCHC), red cell distribution width (RDW), mean corpuscular volume (MCV), mean corpuscular hemoglobin (MCH), hemoglobin concentration (HB)), white blood cell count (WBC) and thrombocytes parameters (platelet count (PLT), mean platelet volume (MPV)). Serum samples collected in separator tubes were utilized for conducting clinical chemistry analyses. The parameters, namely alkaline phosphatase (ALP), aspartate aminotransferase (AST), alanine aminotransferase (ALT) and triglyceride (TG), total cholesterol (TC), total protein (TP), total bilirubin (TBIL), creatinine, urea, albumin (ALB), uric acid (UA), high density cholesterol (HDL-C), glucose, calcium, and inorganic phosphorus (Phos) were measured using a Mindray BS220 automatic biochemistry analyzer (Shenzhen, China).

Following overnight fasting (with free access to water), the male mice were sacrificed on day 92 and the female mice were sacrificed on day 93 by the method of cervical dislocation. Macroscopic examinations were performed after sacrifice. The weights of the heart, liver, spleen, lung, kidneys, stomach, testis/ovaries were recorded. The relative organ weights (g/g body weight) were determined by using the terminal body weight as the basis for calculation.

Histopathological evaluations were conducted on the heart, liver, spleen, lung, kidneys, stomach, and testes or ovaries. The organs were first fixed in 10 % neutral buffered formalin, followed by embedding in paraffin, sectioning, and staining with hematoxylin-eosin (H&E). Observations of the histopathological changes in these organs were carried out using an optical microscope (Nikon Eclipse E100, Japan) equipped with an imaging system (Nikon DS-U3, Japan) in both control and OKGM groups.

2.5. Measurement of SCFAs by gas chromatography (GC)

Mice feces of each cage were collected on day 30, 60, and 90. The feces and crotonic acid (5 mmol/L) were mixed and homogenized in an ice-cold water bath for 1 min, followed by thoroughly mixing under

ultrasonic for 25 min. The mixture was centrifuged at 4 °C with 2500 g for 15 min. The lactate content was determined according to the kit instructions (Abcam, Shanghai, China). The contents of SCFAs including acetic, propionic, butyric, isobutyric acid, valeric acid, and isovaleric acid were measured by gas chromatography according to a previous report with some modifications (Hu, Nie, Li, & Xie, 2013).

2.6. Microbial community analysis

Fecal samples, collected on days 30, 60, and 90 of the study, were rapidly frozen at −80 °C and then dispatched to Shanghai Majorbio Technology Co., Ltd., secured in dry ice, for comprehensive microbiota composition analysis. To extract total bacterial DNA from these samples, we employed the OMEGA-soil DNA Kit (Omega Bio-Tek, Inc., GA, USA), strictly adhering to the provided manufacturer's instructions. The V3-V4 hypervariable regions of the bacterial 16S rRNA gene were amplified through PCR, utilizing forward primer 338F (5′-ACTCCTACGGGAGG-CAGCAG-3′) and reverse primer 806R (5′-GGACTACHVGGGTWTC-TAAT-3′). Subsequent sequencing was conducted on the Illumina MiSeq PE300 platform, generating paired-end reads of 2 × 300 bp. The sequence data and bioinformatics analysis were processed using the Quantitative Insights into Microbial Ecology (QIIME) 1.9 platform, with further analysis conducted on the Majorbio I-Sanger Cloud Platform.

2.7. Statistical analysis

Research data were expressed as mean ± standard deviation. One-way analysis of variance (ANOVA) followed by a Tukey's post hoc test was used to analyze the significant difference among various groups. The significance level of $p < 0.05$ was used in all comparisons.

3. Results and discussion

3.1. Body weight gains and feed conversion analysis

As shown in Fig. S2, the weekly weight gain of the LOKM had no significant difference with the CM group during 13 weeks ($p > 0.05$); the LOKF group had a significantly higher weekly weight gain than the CF group only at weeks 4, 5, 9, 12, and 13; MOKM and HOKM groups showed a significantly lower weekly weight gain after week 4 than CM group ($p < 0.05$); MOKF and HOKF groups showed a significantly lower weekly weight gain after week 2 than CF group ($p < 0.05$). This finding suggested that the intake of OKGM decelerated the rate of body weight gain, especially at higher dosages. Numerous studies had demonstrated the effectiveness of glucomannan in facilitating weight loss (Chew & Brownlee, 2018). As shown in Table S2, food conversion trends were similar among groups, decreasing with the extension of feeding time. While not statistically significant ($p > 0.05$), there was a trend towards lower food conversion efficiency in mice receiving medium and high doses of OKGM compared to the control group. The OKGM might control body weight based on the mechanisms of promoting satiety, preventing nutrient absorption and altering gastrointestinal hormone secretion (Kundi et al., 2021; Slavin, 2005). The different weight loss effect of OKGM between female and male might be attributed to inherent hormonal differences, particularly estrogen's role in metabolic regulation, and the gender-specific gut microbiota composition, which can differentially influence the metabolism of dietary fibers and SCFAs production. However, it's important to note that this study did not specifically investigate these mechanistic underpinnings, indicating a valuable direction for future research focused on hormonal and microbiota-related mechanisms.

The daily mean intake of OKGM per kilogram of body weight was determined using the nominal dietary OKGM concentrations, along with feed consumption and body weight data. The values calculated for the low-, medium-, and high-dose groups were 3.40, 6.86, and 10.21 g/kg body weight/day, respectively, for male mice and 3.87, 7.95, and 12.01 g/kg body weight/day, respectively, for female mice. Mice fed OKGM were observed to be in good health and did not show any unusual behavior until being sacrificed. The no-observed-adverse-effect-level (NOAEL) for OKGM was higher than the highest dose tested.

3.2. Hematology and clinical chemistry analysis

No significant differences ($p > 0.05$) were observed in hematological parameters between the control and experimental groups of mice (Table S3). The values obtained for all parameters were within the normal range for mice. Furthermore, there were no significant differences ($p > 0.05$) in clinical chemistry values, including ALP, AST, ALT, TP, TBIL, creatinine, UREA, ALB, UA, HDL-C, glucose, calcium, and Phos, between the control and experimental OKGM groups (Table S4). Therefore, it can be inferred that OKGM had no negative effects on normal liver and kidney function metabolism in healthy mice. Furthermore, it was noteworthy that the TC and TG in HOKM and HOKF were significantly lower than those in control group, the TG in MOKF was significantly lower than that in control group ($p < 0.05$). It suggested that high-dose intake of OKGM may affect fat absorption or metabolism in mice.

3.3. Organ weights and histopathological examination

The relative weights of the empty caecum were found to be significantly higher in both male and female mice of the mid- and high-dose groups ($p < 0.05$) as compared to the control group (Table S5). No significant differences in the weights of other organs were observed between the control group and the mice fed with OKGM. Cecal enlargement commonly occurs in mice consuming substantial amounts of carbohydrates that are poorly digestible or slowly absorbed (Garthoff et al., 2010; Jonker, Hasselwander, Tervila-Wilo, & Tenning, 2010). Microbial fermentation of indigestible carbohydrates occurred in the caecum and colon, resulting in the production of SCFAs. The SCFAs exerted a trophic effect on the intestinal epithelium and were thought to contribute to diet-induced cecal enlargement (Sakata, 1986). Increased osmolarity of cecal contents and increased bulk of contents were some of the other potential mechanisms that could contribute to cecal enlargement (Jonker, Fowler, Albers, Tzoumaki, van het Hof, & Aparicio-Vergara, 2020). The OKGM belonged to the indigestible, fermentable carbohydrate. Soft feces or diarrhea, which is commonly observed in animals that consume large amounts of indigestible carbohydrates, was not observed in mice that were fed with OKGM. The cecal enlargement that resulted from the ingestion of indigestible carbohydrates was not considered a toxicological concern in general.

Based on the histological examination of the heart, liver, spleen, lung, kidney, stomach and testes/ovaries, there were no pathological changes related to the administration of OKGM (Fig. S3). The gross pathological observation revealed no differences between the control and OKGM groups.

3.4. Analysis of SCFAs contents in mice feces

The SCFAs are crucial for maintaining the structure and function of intestinal tissue. Previous research, as reported by Zhang et al. (2021), indicated that KGM enhanced the production of SCFAs, thereby improving gut microbiota health. The Fig. 1 and Fig. S4 illustrated the dynamic fluctuations in SCFAs and lactate concentrations in mouse feces over time (30, 60, and 90 days). There appeared to be a positive correlation between these concentrations and the age and body weight of the mice. Notably, in the HOKM and HOKF groups, total SCFA and lactate levels were significantly elevated compared to the control groups on all three measurement days ($p < 0.05$). However, such an increase in the LOKM and LOKF groups was only significant on day 90 ($p < 0.05$). Remarkably, acetic acid, a major constituent of SCFAs, was considerably higher in the MOKM, MOKF, HOKM, and HOKF groups than in the

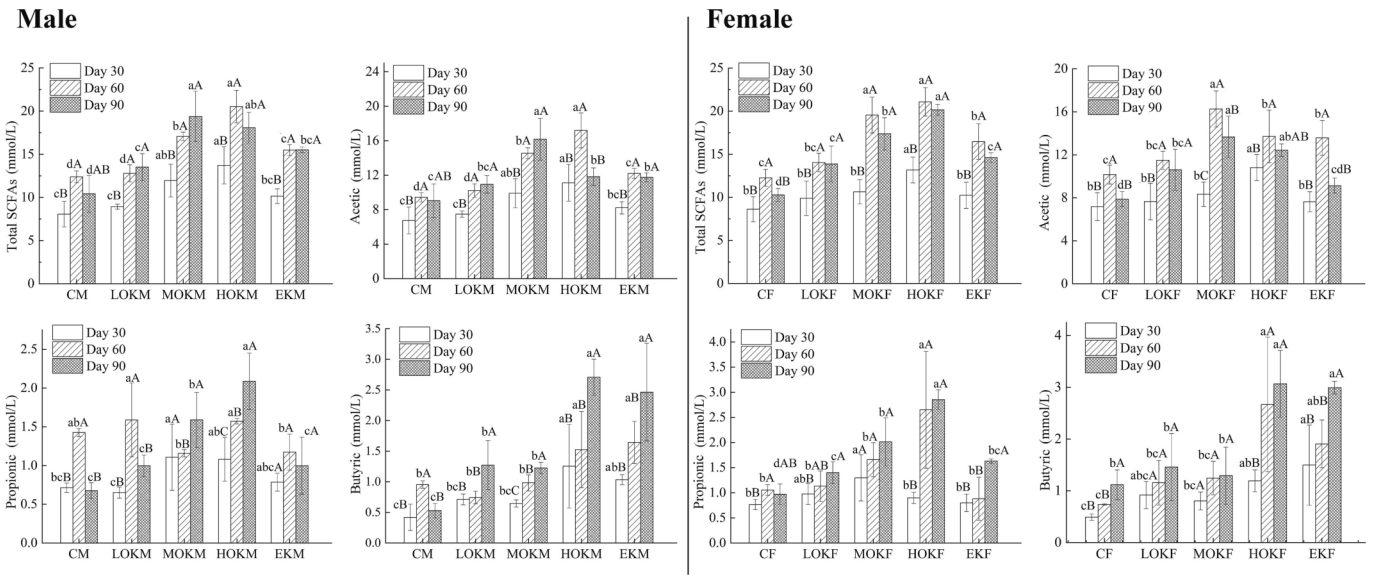

Fig. 1. Temporal Dynamics of SCFAs content in mice feces at different time (30, 60 and 90 days). Statistical differences between groups at the same time point are denoted by lowercase letters (a-d), while significant changes within the same group across different time points are indicated by uppercase letters (A-C).

control groups at day 60 and 90 ($p < 0.05$), with an exception noted for the LOKF group at day 30 and 60.

Comparatively, acetic acid levels in the EKM and EKF groups surpassed those in the control groups on day 60 and 90, yet were significantly lower than in the MOKM and MOKF groups ($p < 0.05$). When compared to control groups, propionic acid levels were notably higher in the MOKF and MOKM groups on day 30, in the HOKF groups on day 60, and in both the HOKM and HOKF groups on day 90 ($p < 0.05$). This suggests that OKGM fosters a greater increase in acetic and propionic acids than EKGM at the same intake level. Interestingly, butyric acid levels in the HOKM, HOKF, EKM, and EKF groups were significantly higher than those in the control groups at varying times ($p < 0.05$), but only in the LOKM and MOKM groups was this significant on day 90. This indicates that EKGM is more effective than OKGM in enhancing butyric acid production at equivalent intake levels. Similarly, isobutyric acid levels were significantly higher in the MOKM, MOKF, HOKM, and HOKF groups than in the control group at 60 and 90 days, and these groups also had higher levels than the EKM and EKF groups. This reveals that increased intake of OKGM leads to greater production of isobutyric acid by the gut microbiota. The levels of valeric and isovaleric acids in the HOKM and HOKF groups on day 90 were significantly higher than those in the control and EKGM groups. This demonstrates that continuous high-dose intake of OKGM enhances the production of these acids by the gut microbiota. Additionally, lactate content in the MOKM and MOKF groups was significantly higher than in the EKGM groups ($p < 0.05$) at 60 and 90 days, showing that OKGM has a more pronounced effect on lactate production than EKGM at the same intake level.

In short, the levels of acetic acid, propionic acid, and lactate in the OKGM groups exceeded those in the EKGM groups at the same intake level, while butyric acid content was higher in the EKGM groups than in the OKGM groups. The varied impacts of OKGM and EKGM on SCFA and lactate production suggest distinct effects on the composition of gut microbiota.

3.5. Gut microbiota composition analysis

3.5.1. Changes in the diversity of gut microbiota

A total of 5,956,581 valid sequences were obtained from 120 fecal samples by high-throughput pyrosequencing after eliminating the unqualified sequences. All the effective reads were clustered into Operational taxonomic units (OTUs) at a 97 % sequence similarity criterion. The Rarefaction and Shannon curves were shown in Fig. S5. The Rarefaction curves almost leveled out with recent sequencing, demonstrating that the amount of sample sequence data was reasonably large for subsequent analysis. The Chao, Ace, Sobs, Shannon and Coverage (Fig. S6) indices were calculated. There was no significant difference in Chao, Ace, sobs and Shannon indexes between the 30-day OKGM groups and the control groups ($p > 0.05$). The Chao, Ace, and sobs indexes of 60- and 90-day OKGM groups tended to be higher than those of the control groups, although they did not show significant differences ($p < 0.05$). This indicated that long-term intake of OKGM slightly increased the richness of gut microbiota in mice. The coverage index for each sample was greater than 99.8 %, which indicated an adequate sequencing depth for the evaluation of the gut microbiota (Tian et al., 2019).

The Principal Coordinates Analysis (PCoA) depicted in Fig. 2 captures the evolution of gut microbiota composition across 30, 60, and 90 days for both genders of mice. On day 30, the microbiota of female (R = -0.0296, P = 0.635) and male mice (R = -0.1069, P = 0.875) demonstrated high homogeneity with no significant separation across treatments. This uniformity suggests that initial microbial communities were largely unaffected by the various dietary interventions. Moving to day 60, a notable separation emerged in male mice (R = 0.3942, P = 0.001), indicative of a significant shift in microbiota composition in response to OKGM and EKGM treatments. Although less dramatic, female mice also began showing significant microbial differentiation (R = 0.1642, P = 0.026). By day 90, the divergence in female mice became more prominent (R = 0.2127, P = 0.005), suggesting a sustained modulation of gut microbiota by the treatments. Conversely, the male mice's microbiota converged slightly, with less significant differences observed (R = 0.065, P = 0.211). Overall, these temporal alterations underscore the differential impact of OKGM and EKGM on the gut microbiome's composition, affirming the hypothesis that prolonged exposure to these treatments leads to discernible regulatory effects on the gut microbiota.

3.5.2. Changes in the bacterial communities at the phylum level

At the phylum level, as illustrated in Fig. 3, the dominant bacterial sequences belonged predominantly to *Firmicutes*, *Bacteroidetes*, and *Actinobacteria*, collectively accounting for over 90 % of the total microbial abundance. The remaining sequences were distributed among lesser-represented phyla such as *Patescibacteria*, *Desulfobacterota*, *Proteobacteria*, *Verrucomicrobiota*, *Deferribacterota*, *Campilobacterota*, and

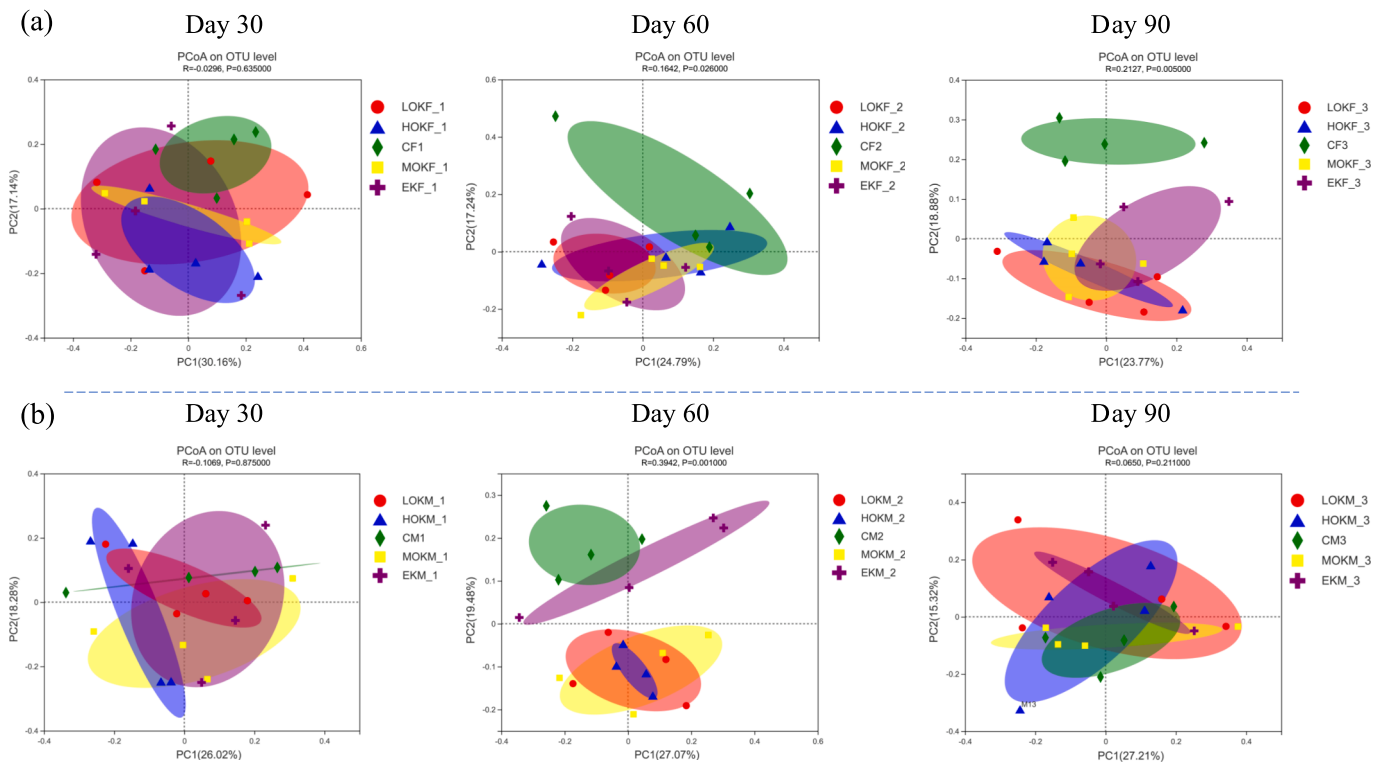

Fig. 2. PCoA plot of different groups. (Note: CM1, LOKM_1, MOKM_1, HOKM_1, and EKM_1 represent the samples of male mice in the control group, low-dose OKGM group, medium-dose OKGM group, high-dose OKGM group, and EKGM group, respectively, at day 30. CM2, LOKM_2, MOKM_2, HOKM_2, and EKM_2 represent the samples of male mice in each group at day 60, while CM3, LOKM_3, MOKM_3, HOKM_3, and EKM_3 represent the samples of male mice in each group at day 90. CF1, LOKF_1, MOKF_1, HOKF_1, and EKF_1 represent the samples of female mice in the control group, low-dose OKGM group, medium-dose OKGM group, high-dose OKGM group, and EKGM group, respectively, at day 30. CF2, LOKF_2, MOKF_2, HOKF_2, and EKF_2 represent the samples of female mice in each group at day 60, while CF3, LOKF_3, MOKF_3, HOKF_3, and EKF_3 represent the samples of female mice in each group at day 90.).

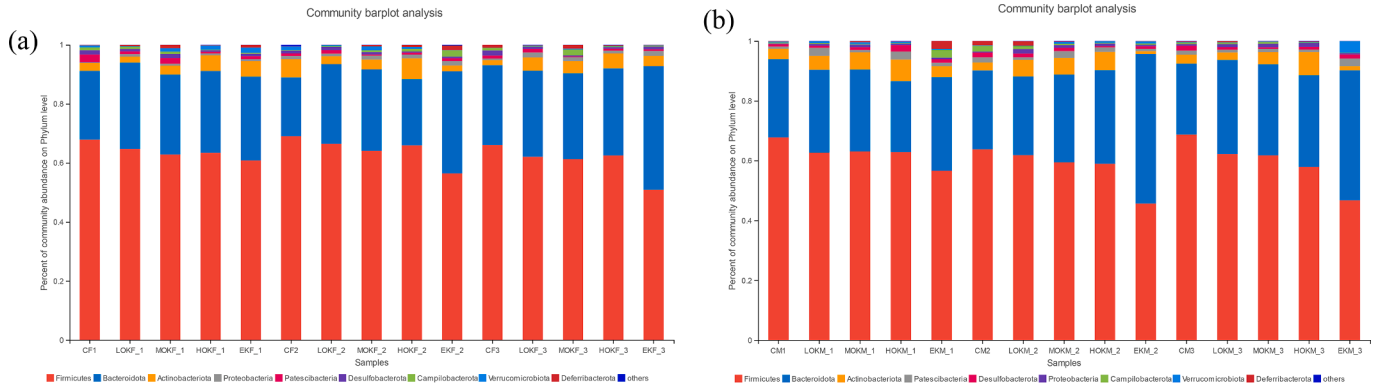

Fig. 3. Bacteria community composition at the phylum level of different groups.

various unclassified bacteria. The dynamic variation in the *Firmicutes* to *Bacteroidetes* ratio (*F/B* value) across different groups is detailed in Table S6. Interestingly, this *F/B* value trend was consistent in both female and male mice, following the sequence: EKGM groups < medium-dose OKGM groups < control groups. Notably, OKGM administration did not demonstrate a clear dose-dependent effect on the *F/B* ratio. In comparison, EKGM groups exhibited a lower *F/B* ratio, potentially due to a decrease in *Firmicutes* and a concurrent increase in *Bacteroidetes* with EKGM intake. Prior studies, such as those by Turnbaugh et al. (2006), have indicated that an elevated *F/B* ratio might enhance the host's fatty acid and energy absorption, potentially leading to weight gain and possibly obesity. Additionally, the relative abundance of *Actinobacteria* was consistently higher in the high-dose OKGM group compared to the others. The abundance of other bacterial phyla was lower and exhibited random dynamic changes over time.

3.5.3. *Changes in the bacterial communities at the genus level*

Fig. 4a and Fig. 4b illustrate the variations in the gut microbiota at the genus level for female and male mice, respectively. Despite the general similarity in bacterial genera across all groups, notable variations in microbial richness were observed. The gut microbiota composition predominantly consisted of genera such as *Lactobacillus*, *Bacteroides*, *Muribaculaceae*, and *Enterococcus*. The *Lactobacillus* genus, in particular, has been extensively recognized for its multifaceted roles, including balancing gut microbiota, boosting immunity, enhancing gut barrier integrity, and possessing antibacterial, anti-inflammatory, and anti-tumor properties. Some *Lactobacillus* species are also integral to the production of fermented foods like yogurt and sauerkraut (Wang, Yao,

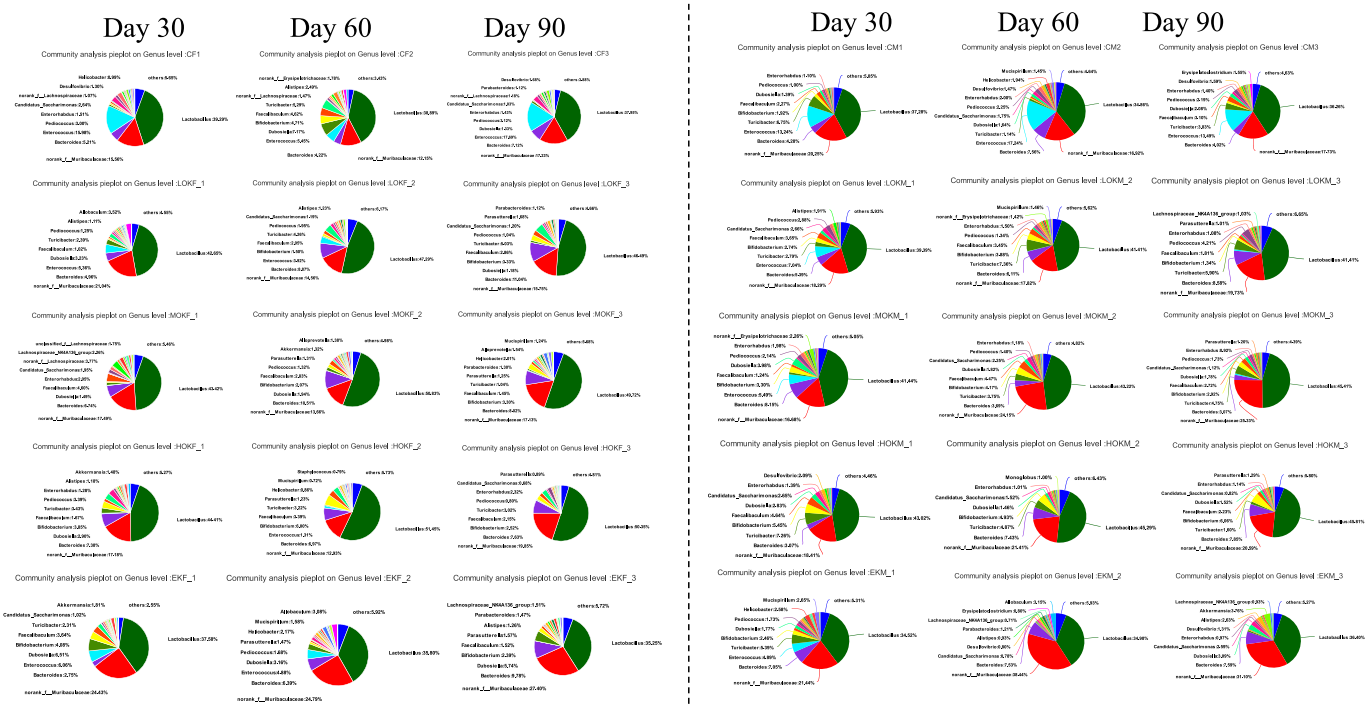

Fig. 4. Bacteria community composition at the genus level of different male group.

Lv, Ling, & Li, 2017). Intriguingly, as depicted in Fig. 6, the proportion of *Lactobacillus* in the control groups (CM and CF) slightly diminished over the course of the study, while in the OKGM groups, it progressively increased, suggesting OKGM's potential to foster *Lactobacillus* growth in the gut microbiota. This increase was more pronounced in the OKGM groups compared to the EKGM groups, with the *Lactobacillus* abundance in the MOKF group rising by 6 % and in the MOKM group by 4 % from day 30 to day 90. This trend indicates that OKGM might be more efficacious than EKGM in augmenting *Lactobacillus* proliferation. Considering *Lactobacillus* as the primary producer of lactate, the elevated levels of lactate in the OKGM groups can be linked to the higher abundance of this genus, as opposed to the EKGM groups. This observation aligns with previous findings that the gut microbiota can convert lactate to propionate (Scheiman et al., 2019), which could elucidate the increased propionate levels observed in the mid-dose OKGM group compared to the EKGM group.

Muribaculaceae, a strictly anaerobic gram-negative bacterial genus within the *Bacteroidetes* phylum, has garnered recent attention due to its successful cultivation and classification (Lagkouvardos et al., 2019). Prevalent in gut microbiota studies involving mouse models, *Muribaculaceae* often emerges as a predominant genus (Park et al., 2021). It's noteworthy that in various studies, *Muribaculaceae* levels tend to diminish in disease models while increasing in healthy controls, suggesting a potential role in maintaining gut health (Dong et al., 2020; Huang et al., 2022). Intriguingly, Sibai and colleagues identified a correlation between *Muribaculaceae* abundance and longevity, noting its heightened presence in fecal samples of long-lived moles (Sibai, Altuntas, Yildirim, Ozturk, Yildirim, & Demircan, 2020). This study revealed dynamic fluctuations in the relative abundance of *Muribaculaceae*, particularly noticeable on day 60 and 90, where its levels were elevated in the OKGM groups compared to controls. This trend, however, did not show a marked dose-dependent response within the OKGM groups. Remarkably, the EKGM groups exhibited a consistently higher *Muribaculaceae* abundance than both the OKGM and control groups across various time points, suggesting that EKGM may more effectively promote *Muribaculaceae* proliferation than OKGM. This finding underscores the distinct microbiota-modulating potentials of these two konjac glucomannan derivatives.

The relative abundance of *Enterococcus* and *Bacteroides* in the gut microbiota ranked just below *Lactobacillus* and *Muribaculaceae*. Notably, the *Enterococcus* genus, comprising facultative anaerobes, is known for its potential to cause infections like urinary tract infections, bacteremia, and endocarditis, especially in immunocompromised individuals (Arias & Murray, 2012; Prieto et al., 2016). Dynamic variations in the *Enterococcus* levels across different timepoints were observed, with notably higher abundances in the control groups compared to both the OKGM and EKGM groups. By day 90, the relative abundance of *Enterococcus* in both OKGM and EKGM samples decreased significantly, aligning closely with each other. This pattern suggests that the consumption of both OKGM and EKGM exerts an inhibitory effect on the proliferation of potentially pathogenic bacteria within the gut ecosystem. Previous research corroborates this finding, revealing that dominant probiotics like *Lactobacillus* can release antagonistic metabolites that suppress the growth of *Enterococcus* (Chen et al., 2019; Divyashree, Anjali, Somashekaraiah, & Sreenivasa, 2021; Monteiro et al., 2019). This evidence highlights the potential of both OKGM and EKGM in modulating gut microbiota towards a healthier composition by restraining pathogenic bacterial growth.

The genus *Bacteroides* played an important role in breaking down complex carbohydrates and producing short-chain fatty acids, which were important for maintaining gut health. However, some species of *Bacteroides* had also been associated with infections in humans, particularly in immunocompromised individuals (Wexler, 2007). The relative abundance of *Bacteroides* in the samples of different time points in male mice showed dynamic changes without a regular trend. In the experimental groups of female mice (LOKF, MOKF, HOKF, and EKF groups), the relative abundance of *Bacteroides* in the samples of day 60 and day 90 was significantly higher than that in the CF group.

The relative abundance of *Bifidobacterium* in the samples at various time points in the male groups (LOKM, MOKM, and HOKM) was significantly higher than that in the CM group. Similarly, in the female groups, the relative abundance of *Bifidobacterium* in the different time point samples of the HOKF group was significantly higher than that in the CF group. This suggests that OKGM may promote the proliferation of

Bifidobacterium in the gut microbiota. In addition, the relative abundance of *Faecalibaculum* in the samples of the MOKM and MOKF groups showed a trend of being higher than that of the EKM and EKF groups. This suggested that OKGM might be more effective than EKGM in promoting the proliferation of *Faecalibaculum* in the gut microbiota. There were references to suggest that the relative abundance of *Faecalibaculum* might have a positive correlation with the production of SCFAs (Wen et al., 2020; Zhang et al., 2015).

3.5.4. Changes in the bacterial communities at the species levels

The visualized Circos plot in Fig. 5 showed the samples from each group at the species level. The top 15 species in relative abundance at the species level were generally consistent among the sample groups for both female and male mice. The two dominant bacterial species were *Lactobacillus_johnsonii* and *uncultured_Muribaculaceae*, and the combined proportion of these two species was higher in the medium and high dose OKGM groups, as well as in the EKGM groups, compared to the corresponding control groups. Possible reasons for the dominant bacterial species in the gut microbiota included: on the one hand, the dominant bacteria had a stronger ability to acquire and utilize OKGM or EKGM, reflecting a growth advantage; on the other hand, the dominant bacteria produced certain antagonistic metabolites during growth and metabolism, thereby inhibiting the growth of other microorganisms (Rooks & Garrett, 2016).

In order to delve deeper into the species-level differences across various groups, a Kruskal-Wallis rank-sum test was applied to the top 15 species based on their relative abundance at the genus level, as illustrated in Fig. 6. We observed dynamic shifts in the species showing significant variations between the groups of female and male mice over the 30, 60, and 90-day intervals. Notably, *Lactobacillus_murinus* emerged as the predominant species showing marked differences among the female groups at 30 days, with its highest abundance recorded in the EKF group, surpassing levels in both the CF and MOKF groups. At 60 days, the dominant differing species were *Lactobacillus_reuteri* and an uncultured *Lactobacillus* specie, with their abundances in the MOKF group significantly outstripping those in the EKF and CF groups. By day 90, *Lactobacillus_reuteri*, *Enterococcus faecium*, and an uncultured *bacterium g_Turicibacter* stood out, with *Lactobacillus_reuteri* showing a notably higher presence in the MOKF group compared to EKF and CF groups, while *Enterococcus faecium* was more abundant in the CF group than in MOKF and EKF groups. A parallel trend was discerned in the male groups. At the 60-day mark, the standout species among the male groups were *Lactobacillus_reuteri*, *Enterococcus_faecium*, *Bifidobacterium_pseudolongum*, and an uncultured_*bacterium_g_Turicibacter*, with *Lactobacillus_reuteri* notably more abundant in the MOKM group than in the CM and EKM groups. The 90-day analysis revealed *Enterococcus faecium*, *Lactobacillus acidophilus*, and *Pediococcus pentosaceus* as the predominant species, with *Enterococcus faecium* displaying a significantly higher level in the CM group compared to MOKM and EKM groups. *Enterococcus faecium*, recognized as a crucial nosocomial pathogen, poses heightened infection risks, especially in immunocompromised patients (Arias et al., 2012; Van Tyne & Gilmore, 2014). In contrast, *Lactobacillus reuteri*, a beneficial gram-positive bacterium, is known for its numerous health benefits, including digestive aid, immune enhancement, and infection prevention (Mu, Tavella, & Luo, 2018). Intriguingly, the control group exhibited a higher relative abundance of *Enterococcus faecium* compared to both OKGM and EKGM groups, whereas *Lactobacillus reuteri* thrived more in the OKGM and EKGM groups than in the control group. This pattern suggests a potential antagonistic relationship between *Lactobacillus reuteri* and *Enterococcus faecium* in the gut, supported by findings that *Lactobacillus reuteri* secretes Reuterin, a broad-spectrum antimicrobial substance, curbing the growth of pathogenic bacteria (Mu et al., 2018). The analysis of intergroup differences further underscores the distinct impacts of OKGM and EKGM on the gut microbiota of mice, particularly highlighting the more favorable influence of OKGM on the proliferation of *Lactobacillus reuteri* within the gut ecosystem.

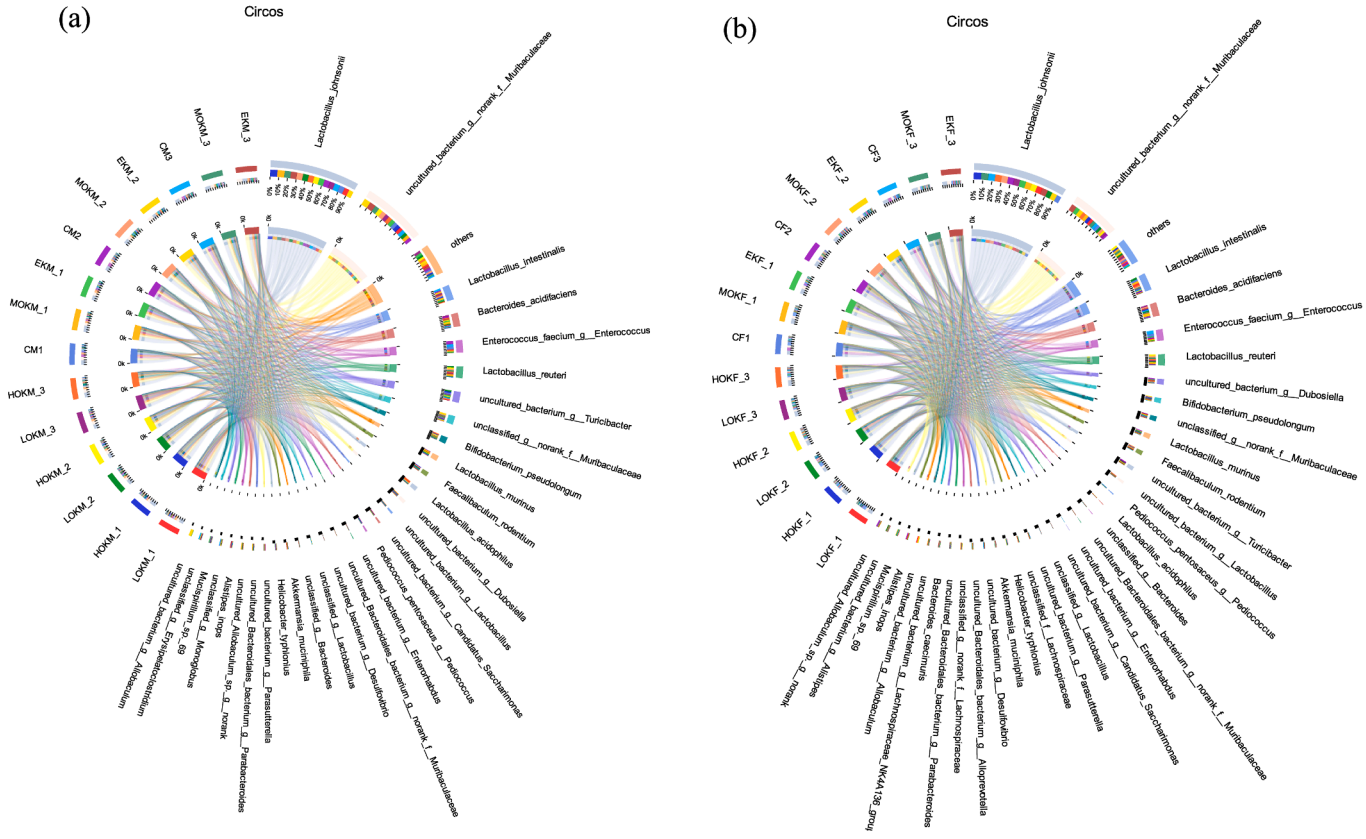

Fig. 5. Circos diagram of bacteria community composition at the species level of male (a) and female (b) groups.

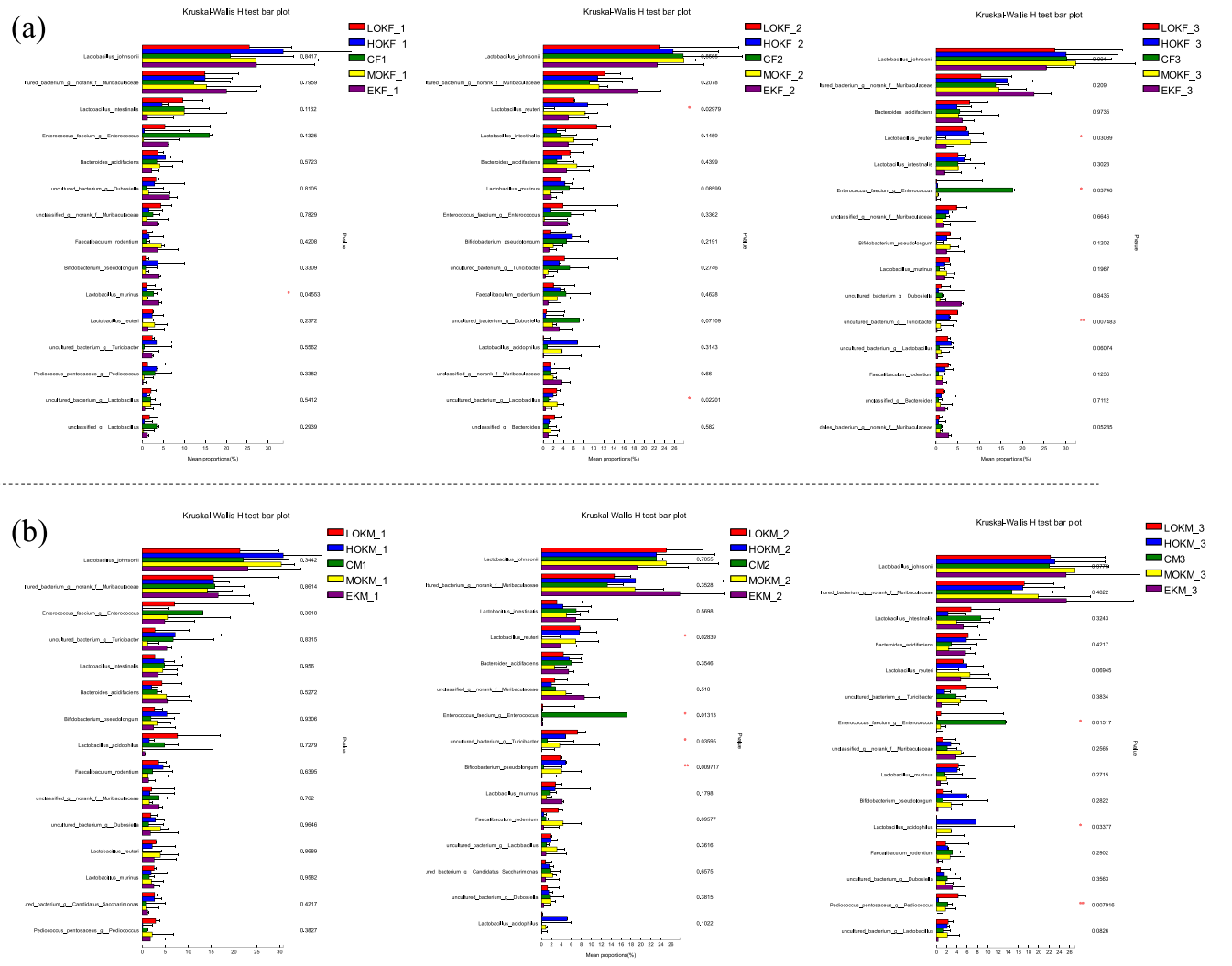

Fig. 6. Kruskal-Wallis rank-sum analysis of the top 15 % microbes at the species level in feces of mice ($p < 0.05$).

The distinct production processes of OKGM and EKGM resulted in notable structural variations, which significantly impacted their interaction with gut microbiota and subsequent metabolic effects. OKGM, synthesized through oxidation, gained additional carbonyl and carboxyl groups. The alteration of chemical groups influenced its solubility and fermentability (Li et al., 2023). Specifically, the presence of these groups in OKGM likely boosted its fermentation by certain bacteria, evidenced by the increased acetate and propionate production and a higher relative abundance of *Lactobacillus*. This suggested that OKGM created an environment conducive to these specific bacteria. EKGM, however, maintained the fundamental functional groups of native KGM but exhibited differences in molecular weight and branching due to enzymatic hydrolysis. This unique structural profile of EKGM influenced the gut microbiota differently than OKGM. It promoted a distinct microbial modulation pattern, characterized by an elevated presence of *Muribaculaceae* and increased butyrate production. This indicated that EKGM served as a selective substrate for different bacterial species or stimulates alternative metabolic pathways within the gut microbiota. Overall, these structural disparities between OKGM and EKGM underscored the intricate relationship between the molecular characteristics of dietary fibers and their biological functionality, particularly regarding gut health and metabolic processes.

4. Conclusion

In conclusion, this study demonstrates that OKGM possesses the potential to be a beneficial functional food additive, as evidenced by several key findings. Firstly, the administration of OKGM to mice did not result in any subchronic toxicity, as indicated by normal food conversion rates, organ indices, hematological parameters, and blood biochemical indices. Pathological and histological examinations further confirmed the absence of significant organ damage across various dosages of OKGM. Notably, OKGM intake, particularly at medium and high doses, was associated with a delay in weight gain, along with a significant reduction in serum triglyceride and total cholesterol levels in the high-dose group. This suggests a potential impact of OKGM on the absorption and metabolism of fats. Moreover, OKGM intake led to an increase in the levels of SCFAs and lactate in mouse feces, with the total content of SCFAs, acetate, and propionate being higher in the OKGM groups compared to the EKGM group, albeit with a lower butyrate content. Importantly, this research highlights the distinctive regulatory effects of OKGM on mouse gut microbiota. Specifically, OKGM consumption resulted in a decreased relative abundance of *Firmicutes* and an increased abundance of *Bacteroidetes*, affecting the *F/B* ratio. Additionally, a notable increase in the relative abundance of *Lactobacillus*, particularly *Lactobacillus reuteri*, was observed, contrasting with the effect of EKGM, which increased the relative abundance of *Muribaculaceae*. These findings collectively underscore the potential of OKGM as a functional food

additive, offering promising avenues for future applications in the food industry.

CRediT authorship contribution statement

Yao Li: Data curation, Investigation, Methodology, Validation, Writing – original draft, Writing – review & editing. **Hongjia Lu:** Funding acquisition, Methodology, Resources, Validation, Writing – review & editing. **Chao Liao:** Data curation, Investigation, Methodology, Resources, Validation. **Xiong Liu:** Conceptualization, Funding acquisition, Project administration, Resources, Supervision, Writing – review & editing.

Declaration of competing interest

The authors declare that they have no known competing financial interests or personal relationships that could have appeared to influence the work reported in this paper.

Data availability

Data will be made available on request.

Acknowledgments

This work was supported by the Natural Science Foundation of Chongqing Science and Technology Commission (grant number: cstc2019jcyj-msxmX0785), the Scientific and Technological Research Program of Chongqing Municipal Education Commission (grant number: KJQN202101309), and the Hainan University Scientific Research Startup Fund Project [grant number: KYQD(ZR)23105].

Research data

The datasets generated during the current study were deposited and are available at the National Center for Biotechnology Information (NCBI), Sequence Read Archive) (SRA) under the accession number PRJNA950552.

Appendix A. Supplementary data

Supplementary data to this article can be found online at https://doi.org/10.1016/j.fochx.2023.101089.

References

Arias, C. A., & Murray, B. E. (2012). The rise of the Enterococcus: Beyond vancomycin resistance. *Nature Reviews Microbiology, 10*(4), 266–278. https://doi.org/10.1038/nrmicro2761

Chen, C. C., Lai, C. C., Huang, H. L., Huang, W. Y., Toh, H. S., Weng, T. C., & Tang, H. J. (2019). Antimicrobial Activity of Lactobacillus Species Against Carbapenem-Resistant Enterobacteriaceae. *Frontiers in Microbiology, 10*. https://doi.org/ARTN 78910.3389/fmicb.2019.00789.

Chen, Y., Zhao, H., Liu, X., Li, Z., Liu, B., Wu, J., & Li, Y. (2016). TEMPO-oxidized Konjac glucomannan as appliance for the preparation of hard capsules. *Carbohydrate Polymers, 143*, 262–269. https://doi.org/10.1016/j.carbpol.2016.01.072

Chew, K. Y., & Brownlee, I. A. (2018). The impact of supplementation with dietary fibers on weight loss: A systematic review of randomised controlled trials. *Bioactive Carbohydrates and Dietary Fibre, 14*, 9–19. https://doi.org/10.1016/j.bcdf.2017.07.010

Divyashree, S., Anjali, P. G., Somashekaraiah, R., & Sreenivasa, M. Y. (2021). Probiotic properties of Lactobacillus casei - MYSRD 108 and Lactobacillus plantarum-MYSRD 71 with potential antimicrobial activity against Salmonella paratyphi. *Biotechnology Reports (Amsterdam, Netherlands), 32*, e00672.

Dong, J., Liang, Q. X., Niu, Y., Jiang, S. J., Zhou, L., Wang, J. M., & Kang, W. Y. (2020). Effects of Nigella sativa seed polysaccharides on type 2 diabetic mice and gut microbiota. *International Journal of Biological Macromolecules, 159*, 725–738. https://doi.org/10.1016/j.ijbiomac.2020.05.042

Espino-Perez, E., Gilbert, R. G., Domenek, S., Brochier-Salon, M. C., Belgacem, M. N., & Bras, J. (2016). Nanocomposites with functionalised polysaccharide nanocrystals through aqueous free radical polymerisation promoted by ozonolysis. *Carbohydrate Polymers, 135*, 256–266. https://doi.org/10.1016/j.carbpol.2015.09.005

Garthoff, J. A., Heemskerk, S., Hempenius, R. A., Lina, B. A. R., Krul, C. A. M., Koeman, J. H., & Speijers, G. J. A. (2010). Safety evaluation of pectin-derived acidic oligosaccharides (pAOS): Genotoxicity and sub-chronic studies. *Regulatory Toxicology and Pharmacology, 57*(1), 31–42. https://doi.org/10.1016/j.yrtph.2009.12.004

Hu, J. L., Nie, S. P., Li, C., & Xie, M. Y. (2013). In vitro fermentation of polysaccharide from the seeds of Plantago asiatica L. by human fecal microbiota. *Food Hydrocolloids, 33*(2), 384–392. https://doi.org/10.1016/j.foodhyd.2013.04.006

Huang, J. M., Liu, D., Wang, Y. W., Liu, L., Li, J., Yuan, J., & Leung, E. L. H. (2022). Ginseng polysaccharides alter the gut microbiota and kynurenine/tryptophan ratio, potentiating the antitumour effect of antiprogrammed cell death 1/programmed cell death ligand 1 (anti-PD-1/PD-L1) immunotherapy. *Gut, 71*(4), 734–745. https://doi.org/10.1136/gutjnl-2020-321031

Jian, W., Tu, L., Wu, L., Xiong, H., Pang, J., & Sun, Y. M. (2017). Physicochemical properties and cellular protection against oxidation of degraded Konjac glucomannan prepared by gamma-irradiation. *Food Chemistry, 231*, 42–50. https://doi.org/10.1016/j.foodchem.2017.03.121

Jin, W., Mei, T., Wang, Y., Xu, W., Li, J., Zhou, B., & Li, B. (2014). Synergistic degradation of konjac glucomannan by alkaline and thermal method. *Carbohydrate Polymers, 99*, 270–277. https://doi.org/10.1016/j.carbpol.2013.08.029

Jonker, D., Fowler, P., Albers, R., Tzoumaki, M. V., van het Hof, K. H., & Aparicio-Vergara, M. (2020). Safety assessment of rhamnogalacturonan-enriched carrot pectin fraction: 90-Day oral toxicity study in rats and in vitro genotoxicity studies. *Food and Chemical Toxicology, 139*. https://doi.org/ARTN 11124310.1016/j.fct.2020.111243.

Jonker, D., Hasselwander, O., Tervila-Wilo, A., & Tenning, P. P. (2010). 28-Day oral toxicity study in rats with high purity barley beta-glucan (Glucagel (TM)). *Food and Chemical Toxicology, 48*(1), 422–428. https://doi.org/10.1016/j.fct.2009.10.034

Korkiatithaweechai, S., Umsarika, P., Praphairaksit, N., & Muangsin, N. (2011). Controlled Release of Diclofenac from Matrix Polymer of Chitosan and Oxidized Konjac Glucomannan. *Marine Drugs, 9*(9), 1649–1663. https://doi.org/10.3390/md9091649

Kundi, Z. M., Lee, J. C. Y., Pihlajamaki, J., Chan, C. B., Leung, K. S., So, S. S. Y., & El-Nezami, H. (2021). Dietary Fiber from Oat and Rye Brans Ameliorate Western Diet-Induced Body Weight Gain and Hepatic Inflammation by the Modulation of Short-Chain Fatty Acids, Bile Acids, and Tryptophan Metabolism. *Molecular Nutrition & Food Research, 65*(1). https://doi.org/ARTN 190058010.1002/mnfr.201900580.

Lagkouvardos, I., Lesker, T. R., Hitch, T. C. A., Galvez, E. J. C., Smit, N., Neuhaus, K., & Clavel, T. (2019). Sequence and cultivation study of Muribaculaceae reveals novel species, host preference, and functional potential of this yet undescribed family. *Microbiome, 7*. https://doi.org/ARTN 2810.1186/s40168-019-0637-2.

Li, J., Li, B., Geng, P., Song, A.-X., & Wu, J.-Y. (2017). Ultrasonic degradation kinetics and rheological profiles of a food polysaccharide (konjac glucomannan) in water. *Food Hydrocolloids, 70*, 14–19. https://doi.org/10.1016/j.foodhyd.2017.03.022

Li, Y., Gong, T., Lu, H., Ma, S., & Liu, X. (2023). In vitro fermentation characteristics of oxidized konjac glucomannan and its modulation effects on gut microbiota. *Food Hydrocolloids, 141*. https://doi.org/10.1016/j.foodhyd.2023.108693

Li, Y., Liu, H., Xie, Y., Shabani, K. I., & Liu, X. (2021). Preparation, characterization and physicochemical properties of Konjac glucomannan depolymerized by ozone assisted with microwave treatment. *Food Hydrocolloids, 119*. https://doi.org/10.1016/j.foodhyd.2021.106878

Lu, M. L., Li, Z. J., Liang, H., Shi, M. X., Zhao, L. H., Li, W., & Li, Y. (2015). Controlled release of anthocyanins from oxidized konjac glucomannan microspheres stabilized by chitosan oligosaccharides. *Food Hydrocolloids, 51*, 476–485. https://doi.org/10.1016/j.foodhyd.2015.05.036

Monteiro, C. R. A. V., do Carmo, M. S., Melo, B. O., Alves, M. S., dos Santos, C. I., Monteiro, S. G., . . . Monteiro-Neto, V. (2019). In Vitro Antimicrobial Activity and Probiotic Potential of Bifidobacterium and Lactobacillus against Species of Clostridium. *Nutrients, 11*(2). https://doi.org/ARTN 44810.3390/nu11020448.

Mu, Q. H., Tavella, V. J., & Luo, X. M. (2018). Role of Lactobacillus reuteri in Human Health and Diseases. *Frontiers in Microbiology, 9*. https://doi.org/ARTN 75710.3389/fmicb.2018.00757.

Park, J. K., Chang, D. H., Rhee, M. S., Jeong, H., Song, J., Ku, B. J., & Kim, B. C. (2021). Heminiphilus faecis gen. nov., sp. nov., a member of the family Muribaculaceae, isolated from mouse faeces and emended description of the genus Muribaculum. *Antonie Van Leeuwenhoek International Journal of General and Molecular Microbiology, 114*(3), 275–286. https://doi.org/10.1007/s10482-021-01521-x

Prieto, A. M. G., van Schaik, W., Rogers, M. R. C., Coque, T. M., Baquero, F., Corander, J., & Willems, R. J. L. (2016). Global Emergence and Dissemination of Enterococci as Nosocomial Pathogens: Attack of the Clones? *Frontiers in Microbiology, 7*. https://doi.org/ARTN 78810.3389/fmicb.2016.00788.

Rooks, M. G., & Garrett, W. S. (2016). Gut microbiota, metabolites and host immunity. *Nature Reviews Immunology, 16*(6), 341–352. https://doi.org/10.1038/nri.2016.42

Sakata, T. (1986). Effects of Indigestible Dietary Bulk and Short Chain Fatty-Acids on the Tissue Weight and Epithelial-Cell Proliferation Rate of the Digestive-Tract in Rats. *Journal of Nutritional Science and Vitaminology, 32*(4), 355–362. <Go to ISI>://WOS:A1986E364500003.

Scheiman, J., Luber, J. M., Chavkin, T. A., MacDonald, T., Tung, A., Pham, L. D., & Kostic, A. D. (2019). Meta-omics analysis of elite athletes identifies a performance-enhancing microbe that functions via lactate metabolism. *Nature Medicine, 25*(7), 1104-+. https://doi.org/10.1038/s41591-019-0485-4

Sibai, M., Altuntas, E., Yildirim, B., Ozturk, G., Yildirim, S., & Demircan, T. (2020). Microbiome and Longevity: High Abundance of Longevity-Linked Muribaculaceae in the Gut of the Long-Living RodentSpalax leucodon. *Omics-a Journal of Integrative Biology, 24*(10), 592–601. https://doi.org/10.1089/omi.2020.0116

Slavin, J. L. (2005). Dietary fiber and body weight. *Nutrition, 21*(3), 411–418. https://doi.org/10.1016/j.nut.2004.08.018

Tian, B. M., Zhao, J. H., An, W., Zhang, J. W., Cao, X., Mi, J. L., & Li, J. X. (2019). Lycium ruthenicum diet alters the gut microbiota and partially enhances gut barrier function in male C57BL/6 mice. *Journal of Functional Foods, 52*, 516–528. https://doi.org/10.1016/j.jff.2018.11.034

Turnbaugh, P. J., Ley, R. E., Mahowald, M. A., Magrini, V., Mardis, E. R., & Gordon, J. I. (2006). An obesity-associated gut microbiome with increased capacity for energy harvest. *Nature, 444*(7122), 1027–1031. https://doi.org/10.1038/nature05414

Van Tyne, D., & Gilmore, M. S. (2014). Friend Turned Foe: Evolution of Enterococcal Virulence and Antibiotic Resistance. *Annual Review of Microbiology, 68*(68), 337–356. https://doi.org/10.1146/annurev-micro-091213-113003

Wang, B. H., Yao, M. F., Lv, L. X., Ling, Z. X., & Li, L. J. (2017). The Human Microbiota in Health and Disease. *Engineering, 3*(1), 71–82. https://doi.org/10.1016/J.Eng.2017.01.008

Wen, J., Ma, L., Xu, Y. J., Wu, J. J., Yu, Y. S., Peng, J., & Li, L. (2020). Effects of probiotic litchi juice on immunomodulatory function and gut microbiota in mice. *Food Research International, 137*. https://doi.org/ARTN 10943310.1016/j.foodres.2020.109433.

Wexler, H. M. (2007). Bacteroides: The good, the bad, and the nitty-gritty. *Clinical Microbiology Reviews, 20*(4), 593-+. https://doi.org/10.1128/Cmr.00008-07

Yin, J. Y., Ma, L. Y., Xie, M. Y., Nie, S. P., & Wu, J. Y. (2020). Molecular properties and gut health benefits of enzyme-hydrolyzed konjac glucomannans. *Carbohydrate Polymers, 237*, Article 116117. https://doi.org/10.1016/j.carbpol.2020.116117

Yu, H., Lu, J., & Xiao, C. (2007). Preparation and properties of novel hydrogels from oxidized konjac glucomannan cross-linked chitosan for in vitro drug delivery. *Macromolecular Bioscience, 7*(9–10), 1100–1111. https://doi.org/10.1002/mabi.200700035

Zhang, J., Guo, Z., Xue, Z. S., Sun, Z. H., Zhang, M. H., Wang, L. F., & Zhang, H. P. (2015). A phylo-functional core of gut microbiota in healthy young Chinese cohorts across lifestyles, geography and ethnicities. *Isme Journal, 9*(9), 1979–1990. https://doi.org/10.1038/ismej.2015.11

Zhang, Q., Zhong, D. A., Ren, Y. Y., Meng, Z. K., Pegg, R. B., & Zhong, G. (2021). Effect of konjac glucomannan on metabolites in the stomach, small intestine and large intestine of constipated mice and prediction of the KEGG pathway. *Food & Function, 12*(7), 3044–3056. https://doi.org/10.1039/d0fo02682d